American Mineralogist, Volume 81, pages 495–504, 1996

Cl-rich biotite and amphibole from Black Rock Forest, Cornwall, New York

ALBERT LÉGER, CAROLYN REBBERT, AND JIM WEBSTER

Department of Earth and Planetary Sciences, American Museum of Natural History, Central Park West at 79th Street, New York, New York 10024-5192, U.S.A.

ABSTRACT

Biotite and amphibole containing up to 4.6 and 5.1 wt% Cl, respectively, are found in gneisses from Black Rock Forest, located within the Hudson Highlands of New York. The area was metamorphosed to granulite facies during the Grenvillian orogeny at ~1100 Ma. Small, subeconomic magnetite deposits coexist with the gneisses.

Cl contents in biotite range from 0.1 to 4.6 wt%. Some individual biotite grains are spectacularly zoned, with Cl contents varying from 1.0 to 4.6 wt% within <20 μm. In zoned biotite, an increase in Cl content correlates with increasing Fe and decreasing Mg, Ti, and F. When data from five specimens are compared, however, Cl contents in biotite show only two strong correlations: Cl contents correlate positively with Fe ($r^2 = 0.75$) and negatively with Ti ($r^2 = 0.84$). Cl and Mg are uncorrelated for the complete dataset but show strong correlation within individually zoned grains ($r^2 = 0.74$). F contents show only one correlation, a positive one with Mg ($r^2 = 0.62$). The structural formula for the most Cl-rich biotite analyzed is $(K_{2.00}Na_{0.02})(Mg_{1.94}Fe_{3.90}Ti_{0.07}Al_{0.04})(Si_{5.85}Al_{2.15})O_{20}(OH_{2.46}F_{0.25}Cl_{1.29})$, as normalized to 24 (O + OH + F + Cl). This biotite is one of the most Cl rich ever reported.

Cl contents in amphibole range from 0.2 to 5.1 wt%. Cl contents correlate positively with $Fe^{2+}/(Fe^{2+} + Mg)$ ($r^2 = 0.84$) and K ($r^2 = 0.70$) and negatively with $Si/(Si + {}^{[4]}Al)$ ($r^2 = 0.49$) and Ti ($r^2 = 0.76$). F contents are uncorrelated with any of the other elements analyzed. The structural formula for the most Cl-rich amphibole, a hastingsite, is $(K_{0.57}Na_{0.31})(Ca_{1.90}Na_{0.10})(Fe^{2+}_{2.69}Mg_{0.90}Mn_{0.03}Ti_{0.06}Fe^{3+}_{1.02}Al_{0.29})(Si_{5.80}Al_{2.20})O_{22}(OH_{0.55}F_{0.07}Cl_{1.38})$, as normalized to 13 octahedral and tetrahedral cations.

In rocks with coexisting amphibole and biotite, Cl partitions preferentially into the amphibole and F partitions preferentially into the biotite. Infiltration of the gneisses by fluids rich in Fe and Cl (perhaps as an $FeCl_2$ compound) could explain the formation of magnetite bodies as well as the Fe- and Cl-enriched phases found in and around Black Rock Forest.

INTRODUCTION

Micas and amphiboles provide a significant mineral reservoir for H_2O, F, and Cl in the Earth's crust. Halogen contents in these phases can yield valuable information about fluid composition during metamorphism (e.g., Munoz and Swenson 1981; Valley et al. 1982; Yardley 1985; Boudreau et al. 1986; Vanko 1986; Sisson 1987; Mora and Valley 1989; Zhu and Sverjenski 1991, 1992), formation of the early crust (e.g., Collerson and Fryer 1978), or genesis of ore deposits (e.g., Helgeson 1969; Crerar and Barnes 1976; Seward 1976; Mutchler et al. 1981). It is also important to know the range of possible halogen contents in these minerals for mass-balance models of element transport down subduction zones.

There have been many studies on F-bearing micas and amphiboles. F has an ionic radius similar to OH (1.31 Å vs. 1.38 Å, respectively) and thus easily replaces OH. It is possible to synthesize fluorine phlogopite, which facilitates the gathering of thermodynamic, structural, and chemical data. Cl ions, however, are much larger (1.81 Å) than OH ions, and Cl replaces OH with difficulty. Few studies report Cl contents because of the minor quantity of Cl in most hydrous minerals. The paucity of data for Cl in natural materials is compounded by the fact that end-member chlorine biotite cannot be synthesized for study (a pure chlorannite of composition $K_2Fe_6Al_2Si_6O_{20}Cl_4$ would contain 12.92 wt% Cl). Incorporation of Cl in micas has been investigated experimentally (e.g., Munoz and Ludington 1977; Munoz and Swenson 1981; Munoz 1984; Volfinger et al. 1985), but the amounts of Cl in experimental products are much lower than the Cl contents in the natural phases reported here.

Natural biotite and amphiboles rarely contain >1 wt% Cl (e.g. Lee 1958; Jacobs and Parry 1979; Gunow et al. 1980; Guidotti 1984; Munoz 1984; Mora and Valley 1989), but a few studies report Cl-rich biotite and amphibole (e.g., Leelanandam 1969a, 1969b; Kamineni et al. 1982; Valley et al. 1982; Morrison 1991; Tracy 1991). The purpose of this paper is to present a new field locality

0003–004X/96/0304–0495$05.00

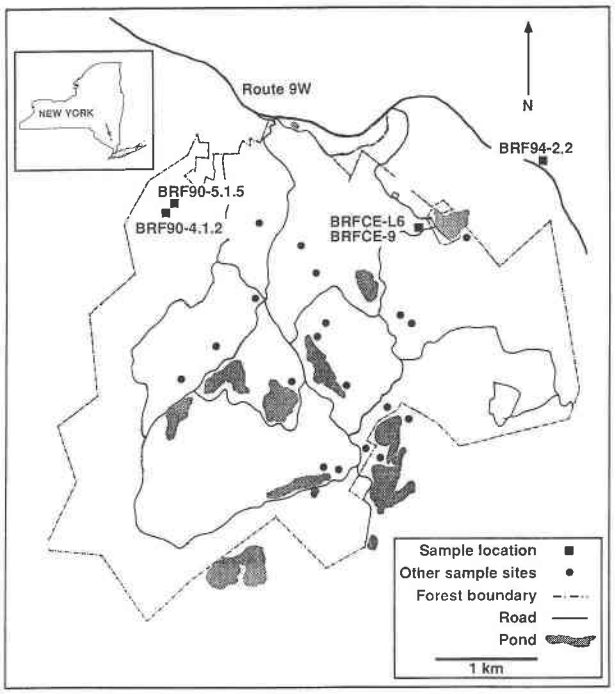

FIGURE 1. Map of the Black Rock Forest, Cornwall, New York, with sample locations.

for Cl-rich biotite and amphibole and to expand the relatively small data base on Cl-rich phases by presenting data on Cl-rich biotite (up to 4.6 wt% Cl) and amphibole (up to 5.1 wt% Cl) from granulite-facies gneisses in and around the Black Rock Forest in the Hudson Highlands of New York.

GEOLOGIC SETTING

Samples were collected in gneisses that crop out in and around the Black Rock Forest, located near Cornwall, New York, about 60 km north of New York City (Fig. 1). Black Rock Forest is located within a narrow belt of crystalline metamorphic rocks known as the Hudson Highlands. This is part of a larger metamorphic belt of Middle Proterozoic rocks that constitute the Adirondack, Green, and Berkshire Mountains of the northern Appalachians and the Blue Ridge Belt of the southern Appalachians (Aleinikoff and Grauch 1990).

Metamorphic rocks of the Hudson Highlands range in age from ca. 960 to 1300 Ma and are derived from limestones, sandstones, and volcanic rocks that were metamorphosed to upper amphibolite and granulite facies during the Grenville orogeny (Helenek and Mose 1984; Aleinikoff and Grauch 1990; Isachsen and Gates 1991). These metasedimentary and metavolcanic units were buried to depths of 25–30 km and subjected to temperatures of 750–800 °C (Dallmeyer and Dodd 1971; Jaffe and Jaffe 1973; Hall et al. 1975; Isachsen and Gates 1991). This resulted in sequences of paragneiss units that include marbles and metapelites, orthogneisses that consist of metamorphosed rhyolitic to basaltic volcanic rocks, and quartzo-feldspathic units for which the protoliths are poorly known (Johnson 1990). These sequences are intruded by numerous granitic rocks; pegmatoidal gneisses and migmatite are also common in the region (Aleinikoff and Grauch 1990). Subsequent metamorphism and deformation occurred during the Taconic, Acadian, and Alleghenian orogenies (Isachsen and Gates 1991).

The Grenvillian gneisses of this region contain an abundance of magnetite deposits, many of which were mined for iron in the eighteenth and nineteenth centuries (Ransom 1966). The magnetite bodies range in size from small sub economic concentrations of magnetite-bearing gneiss, like those at Black Rock Forest, to deposits that produced more than two million tons of iron ore. The deposits consist of magnetite-bearing gneisses, pyroxene skarns, and hydrothermally altered, pegmatoidal leucogneiss (Sims 1958; Collins 1969a, 1969b). The ore mineralogy is monotonously simple with magnetite as the principal iron-bearing phase and lesser amounts of pyrrhotite, pyrite, and hematite.

METHODS OF INVESTIGATION

All data were acquired with an ARL-SEMQ electron microprobe with nine wavelength-dispersive spectrometers at the American Museum of Natural History in New York City. Samples were analyzed at 15 kV operating voltage and 20 nA sample current as measured on brass. On-peak counting times were 20 s. Data were reduced using the CITZAF $\phi(\rho z)$ matrix correction routines (Armstrong 1989) within the PROBE software (Donovan et al. 1992). Standards for all major elements were well-characterized natural silicates or synthetic materials. The following natural standards were used: hornblende for Si, Ti, Al, and Mg; fayalite for Fe; rhodonite for Mn; diopside for Ca; orthoclase for K; albite for Na; and scapolite for Cl. Synthetic compounds were MgF_2 for F and $MgCr_2O_4$ for Cr.

The standard for Cl was a scapolite with 2.74 wt% Cl. Because some of the minerals analyzed contained >5 wt% Cl, extrapolation from the scapolite standard was needed. To check the validity of the extrapolation routine, we analyzed reagent-grade KCl (47.55 wt% Cl) as an unknown with scapolite as the Cl standard. Analyses of KCl gave 48.41 wt% Cl, which is within 2% (relative) of its true value. We also used KCl as the Cl standard and reanalyzed some Cl-rich biotite and amphibole. Results for Cl that used KCl as the standard were also within 2% (relative) of Cl contents analyzed with scapolite as the standard. We therefore conclude that using the scapolite standard was appropriate for all minerals analyzed in this study, and we estimate the analytical error in Cl contents reported in this study at ±2% (relative).

Tests were also performed to check for possible volatilization of Cl in standards and unknowns. A focused electron beam under the same conditions as those used

TABLE 1. Mineral assemblages in five specimens from Black Rock Forest

	BRFCE-9	BRFCE-L6	BRF90-4.1.2	BRF94-2.2	BRF90-5.1.5
Amphibole	X	X	X	X	X
Biotite	X	X	X	X	X
Clinopyroxene	X		X		
Orthopyroxene		X		X	X
Ilmenite	X	X	X		X
Magnetite		X			
Sulfides			X		
Quartz		X	X	X	X
Plagioclase	X	X	X	X	X
Potassium feldspar		X		X	X

for mica and amphibole analyses was left stationary, and counts of Cl were recorded every 10 s. No volatilization of Cl was observed during the first 20 s counting times (the duration of an analysis) on the scapolite or KCl standards. Cl counts remained steady for 120 s on the scapolite and 200 s on the KCl before dropping significantly. Cl counts remained steady on biotite and amphibole for over 600 s.

Digital maps showing the intensity of Cl and Fe$K\alpha$ X-rays were produced on the SEMQ microprobe. Counts were collected at 15 KeV and 20 nA by scanning the beam over the specimen, and counts were averaged over a period of 1–2 min acquisition time.

PETROGRAPHY AND CHEMISTRY OF BIOTITE AND AMPHIBOLE

Mineral assemblages in five samples from Black Rock Forest are listed in Table 1. These five rocks are medium- to coarse-grained granulites that are slightly gneissic to nonfoliated granoblastic in texture. They were chosen because they contain coexisting biotite and amphibole, and they show the range in Cl content observed throughout the field area. Other minerals include plagioclase and either clinopyroxene or orthopyroxene. Quartz, alkali feldspar, titanite, sulfides, magnetite, and ilmenite may also be present. Chlorite occurs as an alteration mineral of biotite.

Biotite

Average biotite compositions for four of the five specimens studied are given in Table 2. In these four specimens, zoning within individual phases is minimal. Two individual analyses are listed for the fifth specimen (BRF90-5.1.5) because individual biotite grains in this sample are strongly zoned. Analyses BRF90-5.1.5(L) and BRF90-5.1.5(H) represent the lowest and highest Cl contents, respectively, found in this specimen. All Fe is given as FeO, and all biotite analyses were normalized to 24 (O + OH + Cl + F). The computer program Minfile (Afifi and Essene 1988) was used to normalize all analyses. Molecular proportions of OH and equivalent H_2O contents in biotite were calculated assuming OH = 4 − Cl − F. Data were also normalized to 14 cations excluding Ca, Na, and K to evaluate the uncertainty that arises from normalization schemes. The latter method increases slightly the number of cations and anions, but both schemes give the same halogen-cation correlations discussed below.

TABLE 2. Selected biotite analyses from Black Rock Forest*

No. of analyses	BRFCE-9 15	BRFCE-L6 15	BRF90-4.1.2 9	BRF94-2.2 28	BRF90-5.1.5(L) 1	BRF90-5.1.5(H) 1
SiO_2	37.50	36.64	38.06	35.77	38.20	35.71
TiO_2	5.28	5.16	4.20	4.68	3.88	0.55
Al_2O_3	13.40	14.02	11.95	14.03	11.42	11.32
Cr_2O_3	0.05	0.02	0.02	0.03	0.04	0.00
FeO_{tot}	17.36	19.18	17.64	24.20	16.94	28.49
MnO	0.03	0.03	0.07	0.11	0.06	0.10
MgO	13.05	11.99	14.02	8.58	14.71	7.95
CaO	0.03	0.01	0.02	0.04	0.02	0.03
Na_2O	0.08	0.09	0.05	0.03	0.04	0.07
K_2O	9.27	9.18	9.75	9.04	10.23	9.58
H_2O**	3.21	3.23	2.83	3.27	2.89	2.23
F	1.37	1.05	1.56	0.35	1.63	0.48
Cl	0.41	0.77	1.38	1.53	1.02	4.64
O = F	0.58	0.44	0.66	0.15	0.69	0.20
O = Cl	0.09	0.17	0.31	0.35	0.23	1.05
Total	100.37	100.76	100.59	101.17	100.17	99.90
Si	5.62	5.53	5.75	5.53	5.79	5.85
Al	2.37	2.47	2.13	2.47	2.04	2.15
Ti	0.01	0.00	0.12	0.00	0.17	0.00
T site	8.00	8.00	8.00	8.00	8.00	8.00
Al	0.00	0.03	0.00	0.08	0.00	0.04
Ti	0.59	0.59	0.36	0.54	0.27	0.07
Cr	0.01	0.00	0.00	0.00	0.00	0.00
Fe^{2+}	2.18	2.42	2.23	3.13	2.15	3.90
Mn	0.00	0.00	0.01	0.01	0.01	0.01
Mg	2.92	2.70	3.16	1.98	3.32	1.94
O site	5.69	5.74	5.76	5.75	5.75	5.97
Ca	0.00	0.00	0.00	0.01	0.00	0.01
Na	0.02	0.03	0.02	0.01	0.01	0.02
K	1.77	1.77	1.88	1.78	1.98	2.00
A site	1.80	1.80	1.90	1.80	1.99	2.03
O	20.00	20.00	20.00	20.00	20.00	20.00
OH	3.25	3.30	2.90	3.43	2.96	2.46
F	0.65	0.50	0.74	0.17	0.78	0.25
Cl	0.10	0.20	0.35	0.40	0.26	1.29
X_F†	0.16	0.13	0.18	0.04	0.19	0.06
X_{Cl}†	0.03	0.05	0.07	0.10	0.07	0.32
X_{Fe}‡	0.43	0.47	0.42	0.61	0.39	0.67

Note: L and H in sample numbers refer to Cl-poor and Cl-rich analyses, respectively, for BRF90-5.1.5 (positions shown in Fig. 2a).

* Normalized to 24 (O + OH + F + Cl).

** H_2O calculated on the basis of 4 (OH + F + Cl).

† X_F = F/4, and X_{Cl} = Cl/4.

‡ X_{Fe} = Fe/(Fe + Mg).

In a few analyses (see Table 2), the 24 (O + OH + Cl + F) formula normalization procedure assigned Ti to fill the balance of tetrahedral sites because of insufficient Si + $^{[4]}$Al. Some studies suggest that Ti may replace Si in tetrahedral sites (Farmer and Boettcher 1981), but most researchers place Ti into octahedral sites (cf. Guidotti 1984). It is now recognized, from Mössbauer studies, that Fe^{3+} probably fills any remaining tetrahedral sites (Dyar and Burns 1986; Dyar 1987; Rancourt et al. 1992). Guidotti and Dyar (1991) demonstrated that biotite from a regionally metamorphosed region in northwestern Maine contains 3–14 mol% of total Fe as $^{[4]}Fe^{3+}$, a ratio that, if

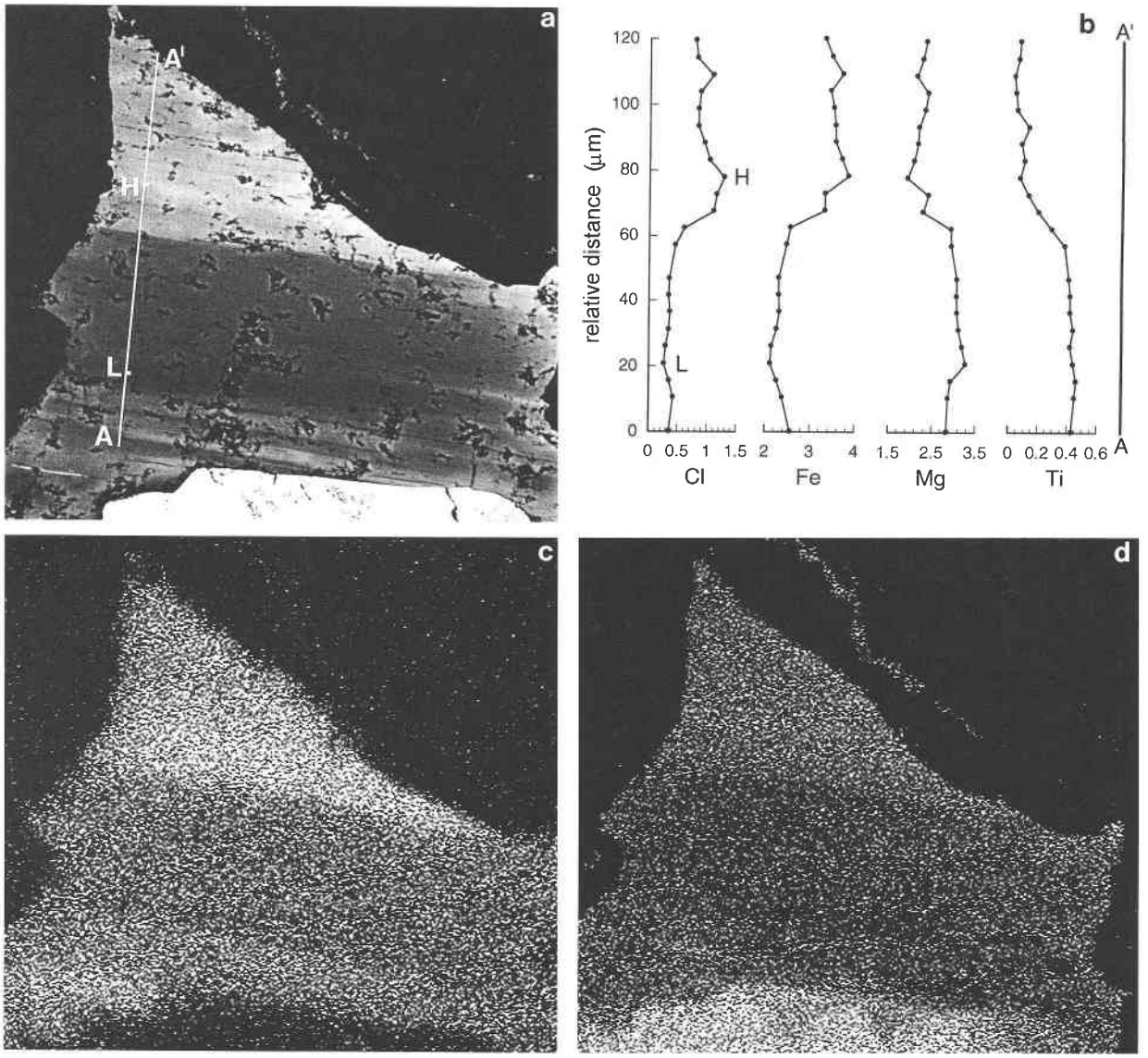

FIGURE 2. Zoned biotite grain in specimen BRF90-5.1.5. (**a**) Back-scattered electron image showing a single biotite grain with a Cl- and Fe-rich region (lighter area) in sharp contact with a Cl- and Fe-poor region (darker area). "L" and "H" represent locations of lowest and highest Cl contents, respectively, in the traverse. The bright phase at the bottom of the figure is ilmenite. (**b**) Electron probe analyses every 5 μm indicate that the major substitutions accompanying Cl incorporation into this biotite structure are an increase in Fe and a decrease in Ti and Mg. Not plotted here is a concomitant decrease in F as Cl increases. (**c** and **d**) Digital Cl and Fe$K\alpha$ X-ray maps showing the positive correlation between Cl and Fe in biotite.

applicable to the present specimens, would provide sufficient $^{[4]}Fe^{3+}$ to fill the tetrahedral sites when normalized to 24 (O + OH + Cl + F).

Significant compositional zoning was observed within individual biotite grains only in specimen BRF90-5.1.5. In a back-scattered electron image of a strongly zoned biotite grain (Fig. 2a), lighter areas (higher mean atomic number) depict Cl- and Fe-rich contents, whereas darker areas represent lower Cl and Fe contents. In this grain, increasing Cl content correlates with increasing Fe and decreasing Mg, Ti, and F. Figure 2b shows a traverse across this zoned biotite grain, giving the number of Cl, Fe, Mg, and Ti atoms per formula unit (apfu). The Cl and Fe$K\alpha$ X-ray maps (Figs. 2c and 2d, respectively) clearly demonstrate the positive correlation between Cl and Fe and the sharp boundary between the Cl-rich and Cl-poor areas. The biotite grain depicted in Figure 2a varies between 1.02 (point L; see analysis in Table 2) and 4.64 wt% Cl (point H, see analysis in Table 2).

Exchange mechanisms for incorporation of Cl into bi-

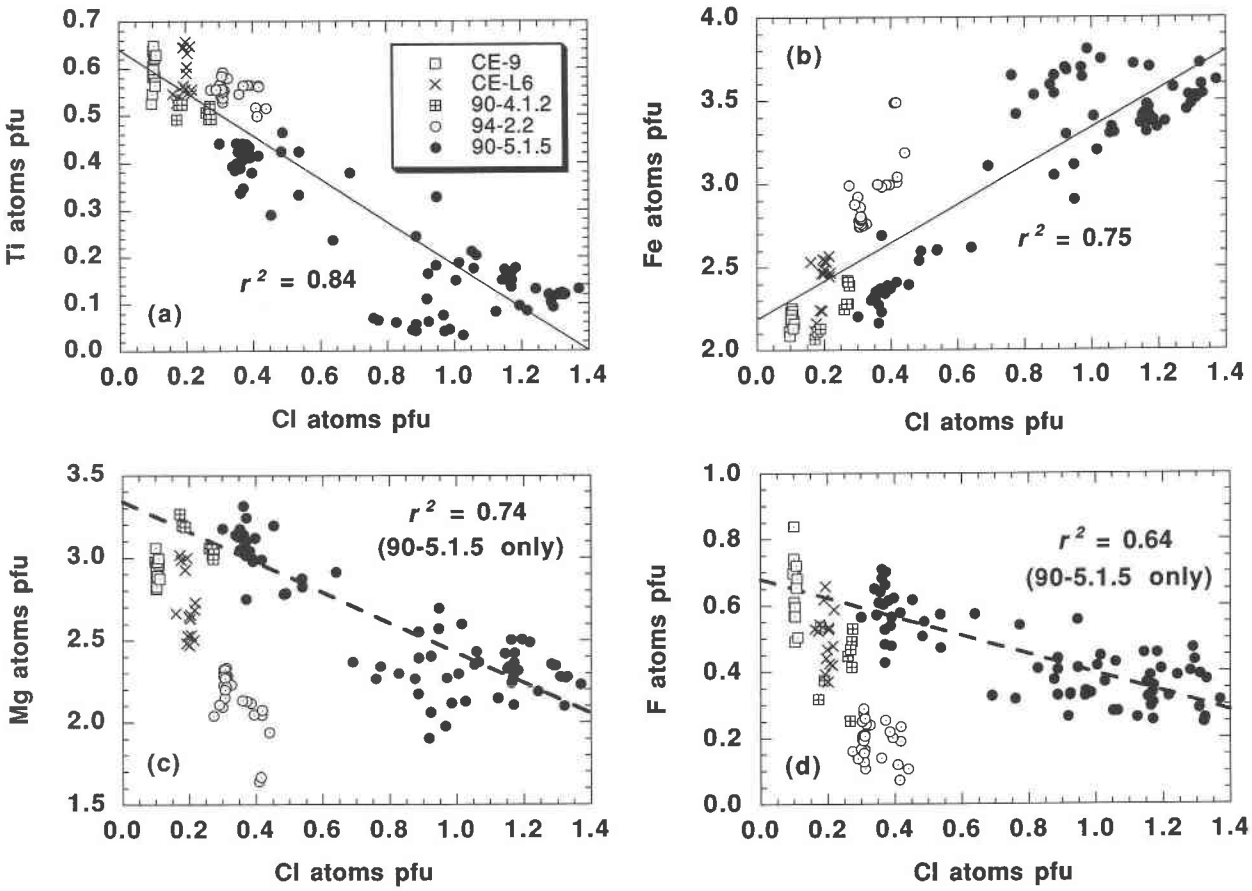

FIGURE 3. Plots of Cl atoms vs. Ti (a) and Fe (b) atoms per formula unit (pfu) in biotite for the entire dataset. The data for only 90-5.1.5, however, show correlations between Cl and Mg (c) and between Cl and F (d).

otite can be evaluated by regression analysis of Cl and other major elements constituting biotite. Listed in Appendix Table 1 are the coefficients of determination (r^2) for Cl vs. other analyzed elements for combined data from all five specimens and for specimen 90-5.1.5 separately. Two strong correlations emerge from the complete dataset when $r^2 > 0.50$: a negative one between Cl and Ti ($r^2 = 0.84$) and a positive one between Cl and Fe ($r^2 = 0.75$) (Fig 3). The correlation between Cl and Ti has not been previously reported to our knowledge. A recent study by Kullerud (1995) found no correlation between Cl and Ti in biotite from granulite-facies gneisses from Norway. Close examination of Figure 3, however, indicates that the correlation between Cl and Ti exists only because of the data from specimen 90-5.1.5. Data from the other four specimens do not show any significant trend between Cl and Ti. This suggests that universal exchange mechanisms for Cl in biotite may not be easily retrieved from small sample sets of natural materials. It is not surprising, then, that the correlations reported here (from five specimens) do not correspond exactly to those from other studies [e.g., Kullerud 1995 (from two specimens)]. Universal exchange mechanisms for Cl incorporation into biotite may be unambiguously retrieved only from laboratory experiments.

The complete dataset used here gives only a weak correlation between Cl and Mg ($r^2 = 0.23$), a result inconsistent with earlier studies (e.g., Munoz and Swenson 1981; Volfinger et al. 1985; Kullerud 1995). There is, however, a good correlation between Cl and Mg when data from only specimen 90-5.1.5 are used ($r^2 = 0.74$). As with Mg, F is uncorrelated with Cl in the complete dataset or ($r^2 = 0.09$) but shows a good negative correlation in specimen 90-5.1.5 ($r^2 = 0.64$). There is a significant positive correlation between F and Mg ($r^2 = 0.62$). The above correlations suggest that the exchange between Fe and Mg in the biotite samples reported here does not follow a simple $MgFe_{-1}$ mechanism.

Amphibole

Average amphibole compositions for four of the five samples studied are given in Table 3. Two analyses (C and D) are given for BRF90-5.1.5 because this specimen has zoned amphibole coexisting with zoned biotite. Although Fe is analyzed on the microprobe as FeO, Fe content in Table 3 is presented as FeO and Fe_2O_3 after nor-

TABLE 3. Selected amphibole analyses from Black Rock Forest*

No. of analyses	BRFCE-9 15	BRFCE-L6 15	BRF90-4.1.2 26	BRF94-2.2 18	BRF90-5.1.5-C 1	BRF90-5.1.5-D 1
SiO_2	42.23	39.13	40.45	39.68	37.09	35.65
TiO_2	2.20	1.87	1.32	2.12	1.22	0.45
Al_2O_3	10.60	12.49	11.13	11.37	12.36	13.02
Cr_2O_3	0.07	0.01	0.04	0.07	0.10	0.04
Fe_2O_3**	3.56	5.60	4.78	6.03	9.34	8.37
FeO	13.93	15.84	15.68	15.21	16.48	19.80
MnO	0.13	0.12	0.12	0.30	0.22	0.21
MgO	10.61	7.84	8.77	7.76	5.70	3.73
CaO	11.57	11.42	11.57	10.89	10.56	10.89
Na_2O	1.87	1.44	1.66	1.44	1.42	1.31
K_2O	1.53	2.16	1.82	1.78	2.57	2.74
H_2O†	1.52	1.37	1.16	1.42	0.85	0.51
F	0.73	0.39	0.37	0.26	0.42	0.14
Cl	0.51	1.55	2.40	1.53	3.33	5.00
O = F	0.31	0.16	0.16	0.11	0.18	0.06
O = Cl	0.12	0.35	0.54	0.35	0.75	1.13
Total	100.66	100.71	100.58	99.41	100.74	100.68
Si	6.33	6.02	6.23	6.15	5.87	5.80
Al	1.67	1.98	1.77	1.85	2.13	2.20
T site	8.00	8.00	8.00	8.00	8.00	8.00
Al	0.21	0.28	0.24	0.23	0.18	0.29
Fe^{3+}	0.40	0.65	0.55	0.70	1.11	1.02
Ti	0.25	0.22	0.15	0.25	0.15	0.06
Cr	0.01	0.00	0.01	0.01	0.01	0.01
Mg	2.37	1.80	2.01	1.79	1.34	0.90
Fe^{2+}	1.75	2.04	2.02	1.97	2.18	2.69
Mn	0.02	0.02	0.02	0.04	0.03	0.03
M1,M2,M3	5.00	5.00	5.00	5.00	5.00	5.00
Ca	1.86	1.88	1.91	1.81	1.79	1.90
Na	0.14	0.12	0.09	0.19	0.21	0.10
M4	2.00	2.00	2.00	2.00	2.00	2.00
Na	0.40	0.31	0.40	0.24	0.23	0.31
K	0.29	0.42	0.36	0.35	0.52	0.57
A site	0.70	0.73	0.76	0.60	0.75	0.88
O	22.00	22.00	22.00	22.00	22.00	22.00
OH	1.52	1.41	1.19	1.47	0.90	0.55
F	0.35	0.19	0.18	0.13	0.21	0.07
Cl	0.13	0.40	0.63	0.40	0.89	1.38
X_F‡	0.18	0.10	0.09	0.06	0.10	0.04
X_{Cl}‡	0.07	0.20	0.32	0.20	0.45	0.69
X^{2+}_{Fe}§	0.42	0.53	0.50	0.52	0.62	0.75
Name‖	magnesian hastingsitic hornblende	magnesian hastingsite	magnesian hastingsite	magnesian hastingsite	magnesian hastingsite	hastingsite

Note: C and D in sample numbers refer to Cl-poor and Cl-rich analyses, respectively, for BRF90-5.1.5.

* Normalized to 13 cations, excluding Ca, Na, and K.

** Fe_2O_3 calculated from charge balance.

† H_2O calculated on the basis of 2 (OH + F + Cl).

‡ $X_F = F/2$, and $X_{Cl} = Cl/2$.

§ $X^{2+}_{Fe} = Fe^{2+}/(Fe^{2+} + Mg)$.

‖ Name according to nomenclature by Leake (1978).

malization to 13 octahedral and tetrahedral cations (M1, M2, M3, and T sites). Cosca et al. (1991) demonstrated that this normalization scheme gives the best approximation to true amphibole compositions. Other normalization procedures (i.e., 23 O atoms or 15 cations excluding Na and K) do not change the main results of this study. Fe^{2+}/Fe^{3+} ratios were calculated from charge balance. Molecular proportions of OH and equivalent H_2O contents in amphibole were calculated with the assumption OH = 2 − Cl − F.

Exchange mechanisms for the incorporation of Cl into the amphibole structure were investigated in a manner identical to that used for biotite. Good positive correlations were observed between Cl and $Fe^{2+}/(Fe^{2+} + Mg)$ ($r^2 = 0.84$) and K ($r^2 = 0.70$), and good negative correlations were observed between Cl and $Si/(Si + {}^{[4]}Al)$ ($r^2 = 0.49$) and Ti ($r^2 = 0.76$) (Fig. 4). F is uncorrelated with any of the other elements analyzed in the amphiboles studied. Appendix Table 2 lists coefficients of determination (r^2) for Cl vs. other analyzed elements for combined data from all five specimens and for specimen 90-5.1.5 separately. There are no major differences in the correlations of the two datasets.

The strong positive correlation between $Fe^{2+}/(Fe^{2+} + Mg)$ and Cl suggests that $FeMg_{-1}$ is an important exchange mechanism accompanying Cl incorporation into amphibole. Oberti et al. (1993) showed that the incorporation of Cl into amphibole deforms the structure, increasing the

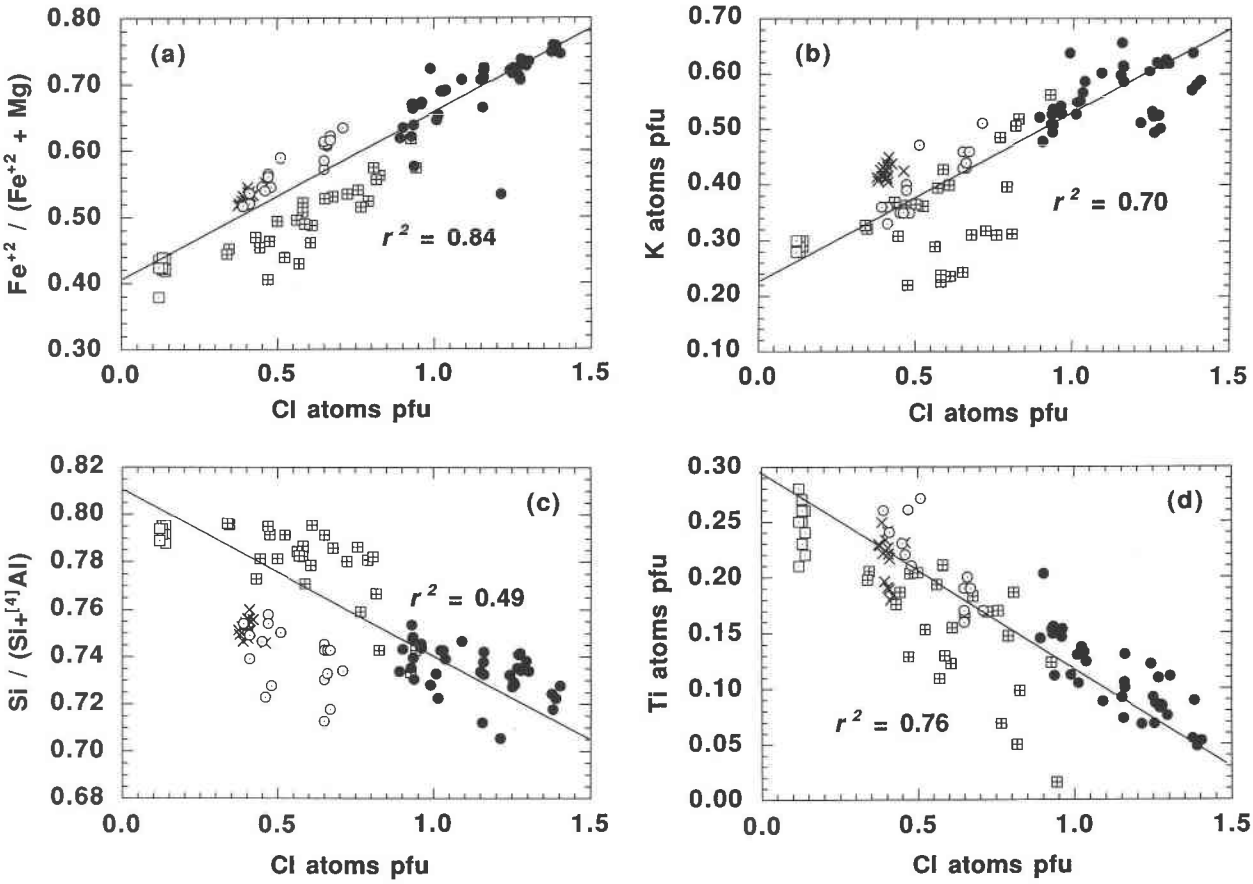

FIGURE 4. Plots of Cl atoms per formula unit (pfu) vs. $Fe^{2+}/(Fe^{2+} + Mg)$ (a), K (b), Si/(Si + $^{[4]}$Al) (c), and Ti (d) in amphibole. Symbols are the same as in Figure 3.

size of the octahedral sites. Fe^{2+} cations preferentially occupy these sites over Mg cations because Fe-Cl bonds are preferred over Mg-Cl bonds (Oberti et al. 1993). Another important positive correlation is between Cl and K. Morrison (1991) argued that in Cl-rich amphiboles, A-site occupancy, particularly by K, influences Cl incorporation. The present data support Morrison's conclusions as well as those of Oberti et al. (1993). The data reported extend the range in Fe and Cl contents reported in those studies, but the exchange relationships remain unchanged at the highest Fe contents.

Cl and F partitioning between coexisting biotite and amphibole can be evaluated by calculating the distribution coefficients ($^{Bio/Amp}K_D$). Only values of apparent $^{Bio/Amp}K_D$ are presented here because mineral compositions do not necessarily reflect equilibrium conditions between biotite and amphibole in all samples. Apparent $^{Bio/Amp}K_D$ values [calculated from analyses in Tables 2 and 3 as $(F/Cl)^{Bio}/(F/Cl)^{Amp}$] for the five specimens studied vary between 1.3 and 7.4 (average = 4.0), which indicates that Cl substitutes for OH preferentially in amphibole over biotite, whereas F substitutes for OH preferentially in biotite over amphibole.

IMPLICATIONS FOR GEOLOGIC HISTORY OF BLACK ROCK FOREST

Biotite and amphibole from the Black Rock Forest area are rich in halogens, especially Cl. On average, amphibole analyses from our sampling of 20 localities within the Forest yield ~1 wt% Cl and ~1 wt% F (unpublished data). The question arises as to what mechanism could account for the increased halogen contents in these particular rocks. Although we are only starting our investigation in this area, we suggest two possible mechanisms for Cl enrichment within gneisses in and around the Black Rock Forest: (1) a Cl-rich protolith, and (2) infiltration of an Fe- and Cl-rich fluid.

The first model presupposes that the protolith to the present gneisses was relatively rich in halogens. Upon prograde metamorphism during the Grenvillian orogeny, the halogens, originally present in low-grade phases, would become progressively enriched in receptive high-grade phases such as biotite and amphibole. This model, analogous to the one in which garnet concentrates Mn in progressively metamorphosed pelites, was described by Guidotti (1984, p. 428) as a possible scenario for the F and

Cl enrichment observed in high-grade rocks in comparison with low-grade rocks. This model is supported by two observations from 90-5.1.5: (1) Cl contents are greatest at the edges of zoned minerals, and (2) the combined modal abundance of biotite and amphibole in this specimen is very low (<5 vol%), thus forcing the few receptive phases available for halogens to be extremely halogen-rich.

The second model suggests that the Fe- and Cl-rich minerals described in this study crystallized in the presence of an Fe- and Cl-rich fluid. The positive correlations between Fe^{2+} and Cl in both biotite and amphibole suggest that a fluid rich in Fe and Cl (perhaps an $FeCl_2$ compound) could have infiltrated the gneisses during metamorphism and exchanged with hydrous minerals. The equilibrium exchange between biotite or amphibole (expressed below as AB) and a Cl- or F-bearing fluid can be expressed as

$$\begin{aligned} &AB(OH) + HCl = AB(Cl) + H_2O, \text{ or} \\ &AB(OH) + HF = AB(F) + H_2O. \end{aligned} \quad (1)$$

On the basis of this model, rock-fluid relationships between Cl-poor and Cl-rich biotite or amphiboles analyzed in rocks from the Black Rock Forest can be written to examine the chemical composition of the equilibrium fluid responsible for element transport to and from reaction sites. For example, the reaction relationship accompanying the transformation of a Cl-poor biotite (analysis L, Table 2) to a Cl-rich biotite (analysis H, Table 2) from specimen 90-5.1.5 is presented as follows:

$$\begin{aligned} &(K_{2.0})(Mg_{3.3}Fe_{2.2}Ti_{0.3})(Si_{5.8}Al_{2.0}Ti_{0.2})O_{20}(OH_{3.0}F_{0.8}Cl_{0.3}) \\ &\quad + (0.1Al^{3+} + 1.7Fe^{2+} + 0.1Si^{4+} + 1.0HCl)_{\text{in fluid}} \\ &\quad = (K_{2.0})(Mg_{1.9}Fe_{3.9}Ti_{0.1})(Si_{5.9}Al_{2.1})O_{20}(OH_{2.5}F_{0.2}Cl_{1.3}) \\ &\quad\quad + (1.4Mg^{2+} + 0.4Ti^{4+} + 0.6HF + 0.5H_2O)_{\text{in fluid}}. \end{aligned} \quad (2)$$

Equation 2 (with formula coefficients rounded to one decimal place) models the reaction between a Cl-poor biotite and an Fe- and Cl-rich fluid to produce a Cl-rich biotite, with Mg, Ti, and F released into the fluid. The same type of reaction can be written for amphiboles. Because amphiboles from specimens CE-9 and 90-5.1.5 follow the same basic trends (see Fig. 4), a rock-fluid reaction relationship relating a Cl-poor amphibole from CE-9 to the amphibole in 90-5.1.5 with the highest Cl content can be written as

$$\begin{aligned} &(K_{0.3}Na_{0.3})(Ca_{1.8}Na_{0.2})(Fe^{2+}_{1.5}Mg_{2.4}Ti_{0.2}Fe^{3+}_{0.7}Al_{0.2}) \\ &\quad \cdot(Si_{6.2}Al_{1.8})O_{22}(OH_{1.5}F_{0.4}Cl_{0.1}) \\ &\quad\quad + (0.3K^{+} + 0.1Ca^{2+} + 1.2Fe^{2+} + 0.3Fe^{3+} \\ &\quad\quad + 0.5Al^{3+} + 0.4Si^{4+} + 1.3HCl)_{\text{in fluid}} \\ &\quad\quad = (K_{0.6}Na_{0.3})(Ca_{1.9}Na_{0.1})(Fe^{2+}_{2.7}Mg_{0.9}Ti_{0.1}Fe^{3+}_{1.0}Al_{0.3}) \\ &\quad\quad\quad \cdot(Si_{5.8}Al_{2.2})O_{22}(OH_{0.6}F_{0.1}Cl_{1.4}) \\ &\quad\quad\quad + (0.1Na^{+} + 1.5Mg^{2+} + 0.1Ti^{4+} \\ &\quad\quad\quad + 0.3HF + 1.0H_2O)_{\text{in fluid}}. \end{aligned} \quad (3)$$

Equation 3 models the increase in Cl content in amphiboles by infiltration of an Fe-Cl fluid (with minor K, Al, and Si), with Mg, and F released into the fluid.

The area in and around Black Rock Forest contains abundant gneisses coexisting with small magnetite deposits. It is possible that during high-grade metamorphism a pervasive fluid flowed through large areas of gneisses of normal or slightly Cl-enriched composition and stripped the rocks of a large integrated quantity of Fe and Cl. Preliminary mapping in the field area shows that the magnetite bodies within Black Rock Forest are aligned with respect to one another. This suggests that ore-bearing fluids were focused into regions of high permeability such as fractures, hinges of folds, or other linear zones of weakness. The channelized fluid then transported significant quantities of ore-forming Fe complexed with Cl to form these localized concentrations of magnetite and Fe- and Cl-rich micas and amphiboles.

Acknowledgments

This study was funded in part by a grant from the Black Rock Forest Consortium. George Harlow kindly reviewed an early version of the manuscript. Many thanks to James Munoz and Jean Morrison for their helpful reviews.

References cited

Afifi, A.M., and Essene, E.J. (1988) Minfile: A microcomputer program for storage and manipulation of chemical data on minerals. American Mineralogist, 73, 446–448.

Aleinikoff, J.N., and Grauch, R.I. (1990) U-Pb geochronologic constraints on the origin of a unique monazite-xenotime gneiss, Hudson Highlands, New York. American Journal of Science, 290, 522–546.

Armstrong, J.T. (1989) CITZAF: Combined ZAF and phi-rho (Z) electron beam correction programs. California Institute of Technology, Pasadena, California.

Boudreau, A.E., Mathez, E.A., and McCallum, I.S. (1986) Halogen geochemistry of the Stillwater and Bushveld complexes: Evidence for transport of the platinum group elements by Cl-rich fluids. Journal of Petrology, 27, 967–986.

Collerson, K.D., and Fryer, B.J. (1978) The role of fluids in the formation and subsequent development of early continental crust. Contributions to Mineralogy and Petrology, 67, 151–167.

Collins, L.G. (1969a) Host rock origin of magnetite in pyroxene skarn and gneiss and its relation to alaskite and hornblende granite. Economic Geology, 64, 191–201.

——— (1969b) Regional recrystallization and the formation of magnetite concentrations, Dover Magnetite District, New Jersey. Economic Geology, 64, 17–33.

Cosca, M.A., Essene, E.J., and Bowman, J.R. (1991) Complete chemical analyses of metamorphic hornblendes: Implications for normalizations, calculated H_2O activities, and thermobarometry. Contributions to Mineralogy and Petrology, 108, 472–484.

Crerar, D.A., and Barnes, H.L. (1976) Ore solution chemistry: V. Solubilities of chalcopyrite and chalcocite assemblages in hydrothermal solution at 200 °C to 350 °C. Economic Geology, 71, 772–794.

Dallmeyer, R.D., and Dodd, R.T. (1971) Distribution and significance of cordierite in paragneiss of the Hudson Highlands, southeastern New York. Contributions to Mineralogy and Petrology, 33, 289–308.

Donovan, J.J., Rivers, M.L., and Armstrong, J.T. (1992) PRSUPR: Au-

tomation and analysis software for wavelength dispersive electron-beam microanalysis on a PC. American Mineralogist, 77, 444–445.

Dyar, M.D. (1987) A review of Mössbauer data on trioctahedral micas: Evidence for tetrahedral Fe^{3+} and cation ordering. American Mineralogist, 72, 102–112.

Dyar, M.D., and Burns, R.G. (1986) Mössbauer spectral study of ferruginous one-layer trioctahedral micas. American Mineralogist, 71, 955–965.

Farmer, G.L., and Boettcher, A.L. (1981) Petrologic and crystal-chemical significance of some deep-seated phlogopites. American Mineralogist, 66, 1154–1163.

Guidotti, C.V. (1984) Micas in metamorphic rocks. In Mineralogical Society of America Reviews in Mineralogy, 13, 357–467.

Guidotti, C.V., and Dyar, M.D. (1991) Ferric iron in metamorphic biotite and its petrologic and crystallochemical implications. American Mineralogist, 76, 161–175.

Gunow, A.J., Ludington, S., and Munoz, J.L. (1980) Fluorine in micas from the Henderson Molybdenite Deposit, Colorado. Economic Geology, 75, 1127–1131.

Hall, L.M., Helenek, H.L., Jackson, R.A., Caldwell, K.G., Mose, D., and Murray, D.P. (1975) Some basement rocks from Bear Mountain to the Housatonic Highlands. In N.M. Ratcliffe, Ed., New England Intercollegiate Conference, 67th Annual Meeting Guidebook, New York, 1–29.

Helenek, H.L., and Mose, D.G. (1984) Geology and geochronology of Canada Hill granite and its bearing on the timing of Grenvillian events in the Hudson Highlands, New York. Geological Society of America Special Paper, 194, 57–73.

Helgeson, H.C. (1969) Thermodynamics of hydrothermal systems at elevated temperatures and pressures. American Journal of Science, 267, 729–804.

Isachsen, Y.W., and Gates, A.E. (1991) Hudson Highlands and Manhattan Prong. In Y.W. Isachsen, E. Landing, J.M. Lauber, L.V. Richard, and W.B. Rogers, Eds., Geology of New York: A simplified account, p. 45–51. New York State Museum/Geological Survey.

Jacobs, D.C., and Parry, W.T. (1979) Geochemistry of biotite in the Santa Rita Porphyry copper deposit, New Mexico. Economic Geology, 74, 860–887.

Jaffe, H.W., and Jaffe, E.B. (1973) Bedrock geology of the Monroe quadrangle, Orange County, New York. New York State Museum and Scientific Services, Map and Chart Series, 20, 74 p.

Johnson, C.A. (1990) Petrologic and stable isotopic studies of the metamorphosed zinc-iron-manganese deposit at Sterling Hill, New Jersey, 108 p. Ph.D. dissertation, Yale University, New Haven, Connecticut.

Kamineni, D.C., Bonardi, M., and Rao, A.T. (1982) Halogen-bearing minerals from Airport Hill, Visakhapatnam, India. American Mineralogist, 67, 1001–1004.

Kullerud, K. (1995) Chlorine, titanium and barium-rich biotites: Factors controlling biotite composition and the implications for garnet-biotite geothermometry. Contributions to Mineralogy and Petrology, 120, 42–59.

Leake, B.E. (1978) Nomenclature of amphiboles. American Mineralogist, 63, 1023–1052.

Lee, D.E. (1958) A chlorine-rich biotite from Lemhi County, Idaho. American Mineralogist, 43, 107–111.

Leelanandam, C. (1969a) Electron microprobe analyses of chlorine in hornblendes and biotites from the charnockitic rocks of Kondapalli, India. Mineralogical Magazine, 37, 362–365.

——— (1969b) Fluorine and chlorine in the charnockitic hornblendes from Kondapalli, India. Neues Jahrbuch für Mineralogie, 10, 379–383.

Mora, C.I., and Valley, J.W. (1989) Halogen-rich scapolite and biotite: Implications for metamorphic fluid-rock interaction. American Mineralogist, 74, 721–737.

Morrison, J. (1991) Compositional constraints on the incorporation of Cl into amphiboles. American Mineralogist, 76, 1920–1930.

Munoz, J.L. (1984) F-OH and Cl-OH exchange in micas with applications to hydrothermal ore deposits. In Mineralogical Society of America Reviews in Mineralogy, 13, 469–493.

Munoz, J.L., and Ludington, S. (1977) Fluoride-hydroxyl exchange in synthetic muscovite and its application to muscovite-biotite assemblages. American Mineralogist, 62, 304–308.

Munoz, J.L., and Swenson, A. (1981) Chloride-hydroxyl exchange in biotite and estimation of relative HCl/HF activities in hydrothermal fluids. Economic Geology, 76, 2212–2221.

Mutchler, F.E., Wright, E.G., Ludington, S., and Abbot, J.T. (1981) Granite molybdenum systems. Economic Geology, 76, 874–897.

Oberti, R., Ungaretti, L., Cannillo, E., and Hawthorne, F.C. (1993) The mechanism of Cl incorporation in amphibole. American Mineralogist, 78, 746–752.

Rancourt, D.G., Dang, M.-Z., and Lalonde, A.E. (1992) Mössbauer spectroscopy of tetrahedral Fe^{3+} in trioctahedral micas. American Mineralogist, 77, 34–43.

Ransom, J.M. (1966) Vanishing ironworks of the Ramapos, 382 p. Rutgers University Press, New Brunswick, New Jersey.

Seward, T.M. (1976) The stability of chloride complexes of silver in hydrothermal solutions up to 350 °C. Geochimica et Cosmochimica Acta, 40, 1329–1341.

Sims, P.K. (1958) Geology and magnetite deposits of Dover District, Morris County, New Jersey. U.S.Geological Survey Professional Paper, 287, 162 p.

Sisson, V.B. (1987) Halogen chemistry as an indicator of metamorphic fluid interaction with the Ponder pluton, Coast Plutonic Complex, British Columbia, Canada. Contributions to Mineralogy and Petrology, 95, 123–131.

Tracy, R.J. (1991) Ba-rich micas from the Franklin Marble, Lime Crest and Sterling Hill, New Jersey. American Mineralogist, 76, 1683–1693.

Valley, J.W., Petersen, E.U., Essene, E.J., and Bowman, J.R. (1982) Fluorphlogopite and fluortremolite in Adirondack marbles and calculated C-O-H-F fluid compositions. American Mineralogist, 67, 545–557.

Vanko, D.A. (1986) High-chlorine amphiboles from oceanic rocks: Products of highly saline hydrothermal fluids? American Mineralogist, 71, 51–59.

Volfinger, M., Robert, J.L., Vielzeuf, D., and Neiva, A.M.R. (1985) Structural control of the chlorine content of OH-bearing silicates (mica and amphiboles). Geochimica et Cosmochimica Acta, 49, 37–48.

Yardley, B.W.D. (1985) Apatite composition and the fugacities of HF and HCl in metamorphic fluids. Mineralogical Magazine, 49, 77–79.

Zhu, C., and Sverjenski, D.A. (1991) Partitioning of F-Cl-OH between minerals and hydrothermal fluids. Geochimica et Cosmochimica Acta, 55, 1837–1858.

——— (1992) F-Cl-OH partitioning between biotite and apatite. Geochimica et Cosmochimica Acta, 56, 3435–3467.

Manuscript received April 14, 1995
Manuscript accepted November 30, 1995

Appendix Table 1. Coefficients of determination (r^2) between Cl apfu and other major elements analyzed in biotite from Black Rock Forest

	All data*	Data from 90-5.1.5 only*
Si	(+) 0.43	(−) 0.01
Ti	(−) 0.84	(−) 0.71
Al	(−) 0.23	(+) 0.39
Fe	(+) 0.75	(+) 0.81
Mg	(−) 0.23	(−) 0.74
K	(+) 0.40	(+) 0.27
F	(−) 0.09	(−) 0.64

* The symbols (+) and (−) represent positive and negative correlations, respectively.

Appendix Table 2. Coefficients of determination (r^2) between Cl apfu and other major elements analyzed in amphiboles from Black Rock Forest

	All data*	Data from 90-5.1.5 only*
Si	(−) 0.49	(−) 0.24
$^{[4]}$Al	(+) 0.49	(+) 0.24
Si/(Si + $^{[4]}$Al)	(−) 0.49	(−) 0.24
$^{[6]}$Al	(+) 0.00	(+) 0.16
Fe^{3+}	(+) 0.42	(−) 0.00
Ti	(−) 0.76	(−) 0.71
Mg	(−) 0.81	(−) 0.80
Fe^{2+}	(+) 0.71	(+) 0.20
Ca	(+) 0.02	(+) 0.19
Na	(+) 0.03	(−) 0.02
K	(+) 0.70	(+) 0.20
F	(−) 0.34	(−) 0.38

* The symbols (+) and (−) represent positive and negative correlations, respectively.